

# Lattice Formation of Peripherally Charged Star Polymers in Aqueous Solution

Taiichi Furukawa\* and Koji Ishizu\*

Department of Organic Materials and Macromolecules, International Research Center of Polymer Science, Tokyo Institute of Technology, 2-12-1, Ookayama, Meguro-ku, Tokyo 152-8552, Japan

Received August 26, 2002; Revised Manuscript Received October 30, 2002

**ABSTRACT:** Functionalized poly(ethylene oxide) (PEO) stars (arm number  $f = 37$ –149) possessing peripheral tertiary amino groups were prepared by organized polymerization using macromonomers. Subsequently, positive charges were introduced into such peripheral tertiary amino groups by quaternization with methyl iodide. The structural ordering of these functionalized and peripherally charged stars was investigated through small-angle X-ray scattering in aqueous solution. PEO stars without charges ( $f > 72$ ) formed a body-centered-cubic (bcc) structure near the overlap threshold ( $C^*$ ). On the other hand, peripherally charged PEO stars ( $f > 37$ ) formed a lattice of bcc even below  $C^*$ . The results indicate that ionization (electric double layer) of stars results in interparticle interactions giving rise to ordering. These interactions were screened by adding inorganic salt (KI).

## 1. Introduction

Star polymers are characterized as the simplest structure of branched species where all chains are connected to a core of small molecular mass. These polymers have gained increasing interest because of their compact structure and high segment density. Stars with multiarms (the critical number of arms is estimated to be of order  $10^2$ ) are expected to form a crystalline array near the overlap threshold ( $C^*$ ) by Witten et al.<sup>1</sup> Willner et al. investigated the ordering phenomena of stars around the  $C^*$  by means of small-angle neutron scattering (SANS).<sup>2,3</sup> They showed that ordering was very weak for 8- and 18-arm polymers but became stronger with increasing arm numbers.

We investigated the structural ordering of core–shell microspheres (poly[(4-vinylpyridene) (core)–styrene (shell)]) through SAXS and transmission electron microscopy (TEM).<sup>4,5</sup> These microspheres formed the lattice with a bcc structure near the  $C^*$ . While in the bulk of film, this structure changed to a face-centered-cubic (fcc) lattice. The transformation of the lattices from a  $C^*$  threshold into a continuous film for (AB)<sub>n</sub> stars and polyisoprene stars with multiarm is very similar to that for the core–shell microspheres.<sup>6,7</sup> These results indicate that the ordering phenomena of microsphere and stars are universal self-organization for branched polymers.

More recently, we synthesized functionalized PEO stars possessing a tertiary amino group at each arm end. Subsequently, positive charges are introduced into such peripheral tertiary amino groups by quaternization with methyl iodide (CH<sub>3</sub>I).<sup>8</sup> In this case, the peripheral charge numbers of these molecules can be controlled by varying the arm numbers of stars, and stars can behave as nanoscopic polyelectrolyte particles in aqueous solution. The nature of the electrostatic interaction between polyelectrolyte particles has received considerable attention through the years. There are several reports concerning the ordering phenomena of these polyelectrolyte particles such as colloid particles,<sup>9</sup> dendrimers,<sup>10,11</sup> and microgels.<sup>12</sup> So, it is interesting to study the structural ordering of these peripherally charged stars in aqueous solution.

In this article, we present the synthesis of functionalized PEO stars having a tertiary amino group or a positively charged ion at the end of each arm. We also made clear the structural ordering of both functionalized and peripherally charged PEO stars in aqueous solution through the SAXS measurement, varying the polymer concentration, arm number, and concentration of additive inorganic salt.

## 2. Experimental Section

**Synthesis of PEO Stars.** Poly(ethylene oxide) (PEO) macromonomers were synthesized by living anionic polymerization technique under high vacuum. Details concerning the synthesis of such PEO macromonomers have been given elsewhere.<sup>13</sup> In brief, PEO macromonomers were synthesized by ring-opening polymerization of living PEO anions end-capped with styrene oxide using 2-[2-(*N,N*-dimethylamino)ethoxy]ethanol potassium alkoxide as an initiator with methacryloyl chloride in toluene. PEO stars were synthesized by free-radical copolymerization of PEO macromonomers with divinylbenzene (DVB) (Tokyo Kasei Ind., Ltd.; 55% *m/p*-isomer = 2, 45% mixture of ethylstyrene and diethylstyrene) in water at 60 °C for 24 h using 2,2'-azobis[2-(2-imidazolin-2-yl)propane] (VA-061; Wako Pure Chemical Industries, Ltd.) as an initiator in a sealed glass ampule under high vacuum. After polymerization, the crude products were recovered by the freeze–dry method. Unreacted PEO macromonomer was removed from the polymerization products by the precipitation fractionation with a benzene–hexane system at 30 °C.

A combination of gel permeation chromatograph (GPC) with light scattering (LS) detector is very useful for measuring the weight-molecular weight ( $M_w$ ) of branched polymers such as star polymers, since one does not need any isolation procedures to remove unreacted arm polymers. GPC measurements were carried out with a Tosoh high-speed liquid chromatography HLC-8120 equipped with a low-angle laser light scattering (LALLS) detector (LS-8: He–Ne laser with a detection angle of 5°) and refractive index (RI), which was operated with TSK gel G2000H<sub>XL</sub> and two GMH<sub>XL</sub> columns, in series using DMF as the eluent at 40 °C. The conversions of star polymers were determined by the ratio of the peak of the PEO star to the total peak area of the polymerization product in GPC charts. The details concerning the calculation method have been given elsewhere.<sup>14</sup>

**Synthesis of Peripherally Charged PEO Stars.** The quaternization of PEO stars was carried out as follows. The

**Table 1.** Free-Radical Copolymerization Conditions and Results of PEO Macromonomer with DVB<sup>a</sup>

code	feed concentration (mol/L)			[DVB]/[M] (mol/mol)	PEO star			
	10 <sup>3</sup> [M]	10 <sup>3</sup> [DVB]	10 <sup>2</sup> [I] <sup>b</sup>		10 <sup>-5</sup> $\bar{M}_w^c$	$\bar{M}_w/\bar{M}_n^d$	conversion (%)	$f^e$
(MS70) <sub>72</sub>	20	0.05	2	1/400	5.0	1.13	38.1	72.1
(MS61) <sub>37</sub>	20	10	0.2	1/2	2.2	1.24	47.7	36.7
(MS61) <sub>149</sub>	20	20	0.2	1	8.9	1.17	53.6	149

<sup>a</sup> Polymerized in water at 60 °C for 24 h under high vacuum. <sup>b</sup> Concentration of VA-061. <sup>c</sup> Determined by SLS in methanol. <sup>d</sup> Determined by GPC-LALLS in DMF. <sup>e</sup> Number of arms.

PEO star was dissolved in ethanol. A large excess of methyl iodide (CH<sub>3</sub>I) was added to this solution. The resulting mixture was stirred at 40 °C for 24 h. After the reaction, the polymer solution was poured into an excess of hexane. The product (peripherally charged PEO star) was purified three times by reprecipitation from an ethanol solution with hexane.

The degree of quaternization of the PEO stars was determined by Volhard's titration. In brief, the quaternized PEO star was reacted with a large excess of AgNO<sub>3</sub> in aqueous solution. The residual AgNO<sub>3</sub> was titrated by ammonium thiocyanate (NH<sub>4</sub>SCN) using ammonium iron(III) sulfate as an indicator.

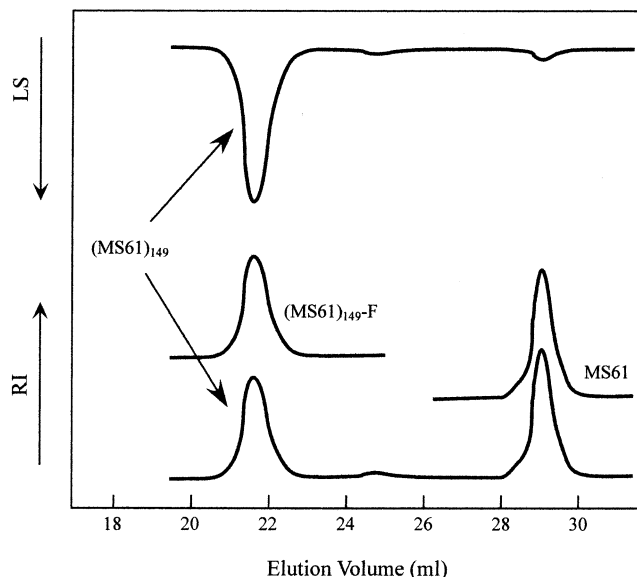
**Dilute-Solution Properties of Stars.** The  $\bar{M}_w$  of the fractionated PEO stars was determined by static light scattering (SLS; Photol TMLS-6000HL; Otsuka Electronics,  $\lambda_0 = 632.8$  nm) in methanol at 25 °C in Zimm mode. The scattering angle was in the range 30°–150°. The RI increment  $dn/dc$  (=0.134 mL/g in methanol) of PEO stars was measured with a differential refractometer (Photol DRM-1021; Otsuka Electronics). Sample solutions were filtered through membrane filters with a nominal pore of 0.2  $\mu$ m just before measurement.

The diffusion coefficient ( $D_0$ ) was determined by the extrapolation to zero concentration on dynamic light scattering (DLS; Otsuka Electronics) data with cumulant method at 25 °C in aqueous solution. The scattering angle was 90°.

**SAXS Measurement.** The SAXS intensity distribution was measured with a rotating-angle X-ray generation (Rigaku Denshi Rotaflex RTP 300RC) operated at 40 kV and 100 mA. The X-ray source was monochromatized to Cu K $\alpha$  ( $\lambda = 1.5418$  Å) radiation. In the measurement of the solution sample, a glass capillary ( $\phi = 2.0$  mm, Mark-Röhrchen Ltd.) was used as a holder vessel. The SAXS patterns were taken with a fine-focused X-ray source using a flat plate camera (Rigaku Denki, RU-100). The SAXS intensity profiles plotted from the horizontal section of the SAXS patterns without considering the smearing correction.

### 3. Results and Discussion

**Synthesis of PEO Stars.** In previous report,<sup>15</sup> we prepared functionalized PEO macromonomers by quenching of living PEO anions with a small amount of glycidyl methacrylate. Subsequently, we carried out free-radical copolymerization of such PEO macromonomers with divinylbenzene (DVB) in water by AIBN as an initiator, varying the feed ratio [DVB]/[M] and the feed concentration of macromonomer [M]. It was found that the conversion of PEO stars formed was very low (conversion < 40%). In this work, free-radical copolymerizations of PEO macromonomers possessing a styrene oxide unit as the spacer with DVB were carried out in water by VA-061 as an initiator. Table 1 lists free-radical copolymerization conditions and results of PEO macromonomer with DVB. Figure 1 shows typical GPC profiles of (MS61)<sub>149</sub> using RI and LS detector. The GPC distribution has a bimodal pattern. The first peak at lower elution volume in RI chart corresponds to the functionalized PEO star. The GPC elution pattern of the second peak is identical with that of the (MS61) macromonomer. Then, copolymerization product (MS61)<sub>149</sub> is a mixture of functionalized PEO star and unreacted PEO macromonomers.

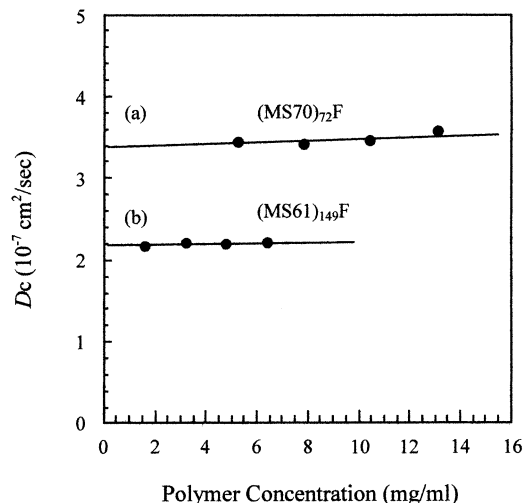
**Figure 1.** GPC profiles of functionalized PEO star (MS61)<sub>149</sub>, star fraction (MS61)<sub>149</sub>F, and PEO macromonomer MS61.

The conversion of star polymer was 53.6%. In no case were cross-linked or insoluble materials observed; it is remarkable that the conversion is high in all the polymerization series in contrast with previous results.<sup>15</sup> Ito and co-workers investigated the micellar copolymerizations of amphiphilic  $\omega$ -methoxy- $\alpha$ -*p*-styrylalkyl PEO macromonomers [methylene units ( $m = 1, 4$ , and  $7$ ) of alkyl sequences] with a limited amount of styrene solubilized therein.<sup>16</sup> The copolymerization rate of styrene was greatly enhanced by the presence of macromonomer micelles, and the rate increased with hydrophobicity (increasing of  $m$ ) of the  $\alpha$ -end group. The characterization of the resulting graft copolymers revealed that the organized copolymerization proceeded in the manner of a pseudo-living radical copolymerization with highly limited terminations between propagating radicals. In our cases also, copolymerization of PEO macromonomers with DVB seems to proceed within micellar domains, because such macromonomers possess a hydrophobic styrene oxide unit adjacent to the terminal double bond. This speculation may be supported by the copolymerization behavior in which cross-linked or insoluble materials have never been observed. Each star (MS-F) was removed from the corresponding unreacted PEO macromonomer by the precipitation fractionation with a benzene–hexane system at 40 °C (see Figure 1). For example, the sample code (MS61)<sub>149</sub>F means  $\bar{M}_w$  of arm =  $6.1 \times 10^3$  and arm number = 149.

**Solution Properties of Stars.** According to the theoretical studies, the ordering phenomena should appear near the overlap threshold ( $C^*$ ).<sup>1</sup> Thus, we examined the dilute solution properties of PEO stars using DLS in water at 25 °C. The observed physical values are listed in Table 2. Figure 2 shows the relationship between translational diffusion coefficient

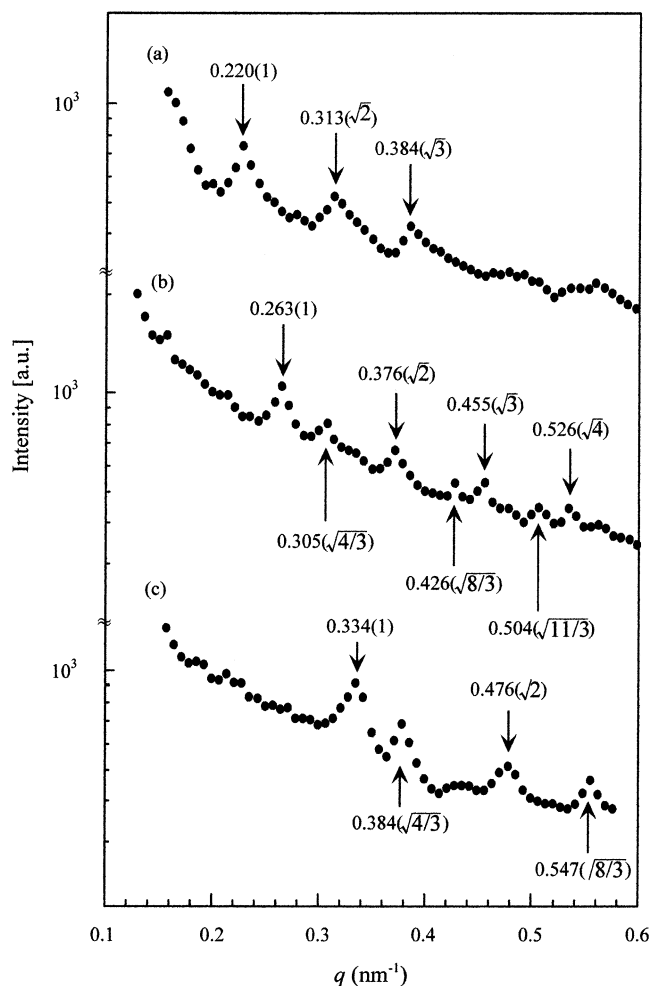
**Table 2. Characteristics of PEO Stars and Peripherally Charged Stars**

code	mol wt		arm no. (no./molecule)	$R_H^c$ (nm)	$C^*^d$ (wt %)
	arm <sup>a</sup> $10^{-3}\bar{M}_n$	star <sup>b</sup> $10^{-5}\bar{M}_w$			
(MS70) <sub>72</sub> F	7.0	5.0	72	$12.6 \pm 0.2$	9.9
(MS70) <sub>72</sub> FI				$12.6 \pm 0.2$	9.9
(MS61) <sub>37</sub> F		2.2	37	$12.7 \pm 0.1$	4.3
(MS61) <sub>37</sub> FI	6.1			$12.2 \pm 0.1$	4.8
(MS61) <sub>149</sub> F		8.9	148	$18.6 \pm 0.2$	5.5
(MS61) <sub>149</sub> FI				$18.7 \pm 0.2$	5.5

<sup>a</sup> Determined by GPC using PEO standard samples with DMF.<sup>b</sup> Determined by SLS in methanol. <sup>c</sup> Determined by DLS in water.<sup>d</sup> Overlap threshold was calculated from equation:  $C^* = 3\bar{M}_w / (4\pi N_A R_H^3)$ .**Figure 2.** Plots of translational diffusion coefficient  $D(C)$  of PEO stars as a function of polymer concentration: (a) (MS70)<sub>72</sub>F; (b) (MS61)<sub>149</sub>F.

$D(C)$  and polymer concentration  $C$  for (MS70)<sub>72</sub>F and (MS61)<sub>149</sub>F. Each  $D(C)$  has an almost constant value. The values of  $D$  for (MS70)<sub>72</sub>F and (MS61)<sub>149</sub>F were  $3.4 \times 10^{-7}$  and  $2.2 \times 10^{-7}$  cm<sup>2</sup>/s, respectively. This suggests that these PEO stars form a single macromolecule in water. Similar tendencies were also observed in (AB)<sub>n</sub> star block,<sup>17</sup> prototype,<sup>18</sup> and double-cylinder type copolymer brushes.<sup>19</sup> The translational diffusion coefficient  $D$  can be estimated by extrapolation of polymer concentration to zero. The Stokes–Einstein's equation  $R_H = kT/6\pi\eta_0 D$ , where  $k$ ,  $T$ , and  $\eta_0$  indicate Boltzmann coefficient, absolute temperature, and viscosity of solvent, respectively. In early report,<sup>20</sup> we judged the shape of PS stars in the solid state through transmission electron microscopy (TEM). It was found from that micrograph that isolated stars showed spherical shape in the solid state. PEO stars seem to be spherical in aqueous solution as well.

Subsequently, the peripherally charged PEO star was converted from the quaternization of the corresponding PEO star having a tertiary amino group at each arm end. Quaternization of functionalized PEO stars with CH<sub>3</sub>I (5-fold amount against tertiary amino groups) was carried out in ethanol. It was found from Volhard's titration that the degree of quaternization was almost 100%. The dilute solution properties of peripherally charged PEO stars in water are also listed in Table 2. It can be seen from Table 2 that the value of  $R_H$  of peripherally charged PEO stars is almost identical compared to corresponding functionalized stars.

**Figure 3.** SAXS intensity profiles for (MS61)<sub>149</sub>F: (a) 9, (b) 28, and (c) 41 wt %.

**Structural Ordering of Functionalized PEO Stars.** The structural ordering of functionalized PEO stars was investigated by means of SAXS in aqueous solution, varying the polymer concentration and arm number. Below  $C^*$ , the star polymer remained isolated, as any arrangement of stars in solution is expected near or above  $C^*$ . We measured first the SAXS intensity profiles of the (MS61)<sub>37</sub>F star at 2 and 8 wt % of aqueous polymer solutions. These polymer concentrations were lower and higher than the  $C^*$  (4.3 wt %), respectively. However, no regular scattering peaks appeared at these concentrations due to disordering.

Figure 3 shows typical SAXS intensity profiles for the (MS61)<sub>149</sub>F, where  $q [= (4\pi/\lambda)\sin\theta]$  (where  $\theta$  is one-half the scattering angle) is the magnitude of the scattering vector. The arrows and the values in parentheses indicate the scattering maxima and interplanar spacing ( $d_1/d_n$ ), respectively, calculated from the Bragg reflection. Below the  $C^*$  (=5.5 wt %), no regular scattering peaks appeared due to disordering. At 9 wt % of polymer concentration (Figure 3a), the first three peaks appear closely at the relative  $q$  positions of  $1:\sqrt{2}:\sqrt{3}$ , as shown in parentheses. The interplanar spacing ( $d_1/d_n$ ) at the scattering angles is relative to the angle of the first maximum according to Bragg's equation:  $2d \sin\theta = n\lambda$  (where  $\lambda = 1.5418$  Å). In general, this packing pattern appears in the lattice of not only simple cubic but also bcc structures. As mentioned in the Introduction, the (AB)<sub>n</sub> and polyisoprene stars with multiarm



**Table 3. Physical Values on Spatial Packing of Cubic Lattices for (MS60)<sub>149</sub>F Star in Aqueous Solution**

polymer concn (wt %)	$q_1^a$ (nm <sup>-1</sup> )	$d_1^b$ (nm)	$D_0^c$ (nm)
4			
0	0.220	28.55	35.00
13	0.235	26.76	27.72
18	0.263	23.86	24.58
23	0.277	22.64	23.00
28	0.313	20.07	29.22
41	0.334	18.79	32.76

<sup>a</sup> Calculated by  $q = 4\pi \sin\theta/\lambda$ . <sup>b</sup> Calculated by  $d_1 = 2\pi/q_1$ .<sup>c</sup> Determined by  $D_0 = (\sqrt{3}/2)d_1$ .

were packed in the lattice of a bcc structure near  $C^*$ .<sup>6,7</sup> The conformation of PEO stars can be regarded as similar to such stars in solution. It is reasonable that these values correspond to the packing pattern of (110), (200), and (211) planes in a bcc structure.

In the SAXS intensity profile at 28 wt % of polymer concentration, the complicated scattering peaks appear as shown in Figure 3b. The first seven peaks appear at the relative  $q$  positions of  $1:\sqrt{4/3}:\sqrt{2}:\sqrt{8/3}:\sqrt{3}:\sqrt{11/3}:\sqrt{4}$ . In general, the relative  $q$  positions of  $1:\sqrt{4/3}:\sqrt{8/3}:\sqrt{11/3}$  correspond to the packing pattern of (111), (200), (220), and (311) planes in a fcc structure. Therefore, it is concluded that the PEO stars were packed in the mixed lattice of bcc and fcc structures at this polymer concentration. Similar mixed lattice patterns are also observed in the SAXS profile at 41 wt % of polymer concentration (Figure 3c). It is noticed that the first peak shift to the side of high  $q$  position in the order of the increment of polymer concentration. This fact means that Bragg spacing  $d_1$  became shorter with increasing the polymer concentration.

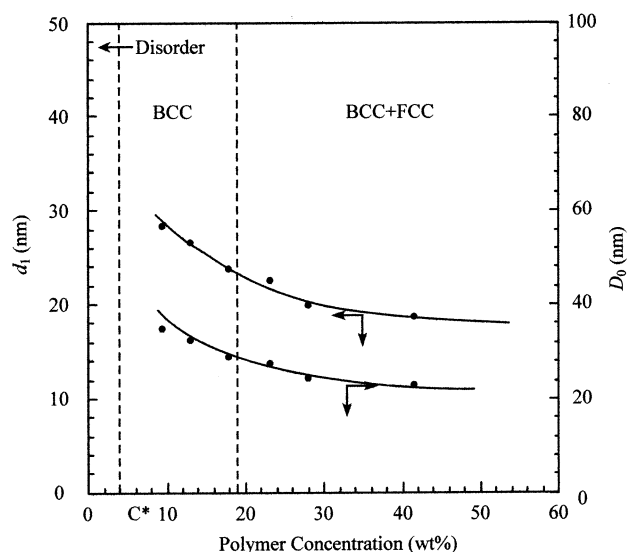
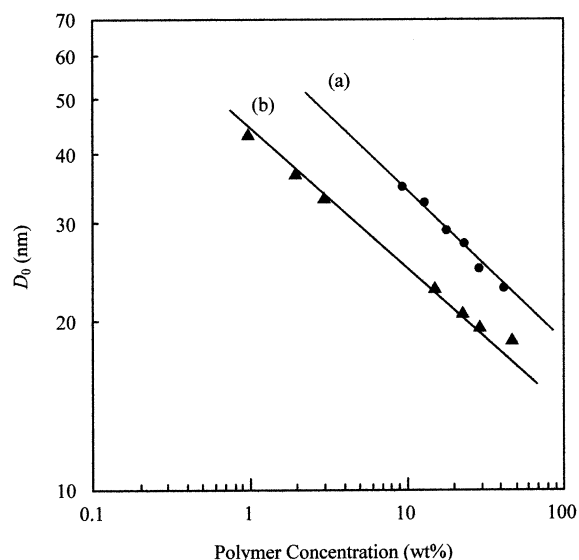
The result of SAXS data obtained for (MS70)<sub>72</sub>F star was almost the same as those for the (MS60)<sub>149</sub>F star. That is to say, the polymer solution below  $C^*$  showed disordering. The structural ordering such as a bcc lattice appeared near  $C^*$ , and this structure changed to the mixed lattice of bcc and fcc with increasing the polymer concentration.

We consider special packing of the cubic lattice in aqueous solution. The measured Bragg spacing  $d_1$  is related to the cell edge  $a_c$  of the cubic lattice and the nearest-neighbor distance of the spheres  $D_0$ :

$$D_0 = (\sqrt{3}/2)a_c = \sqrt{(3/2)}d_1 \quad \text{for bcc} \quad (1)$$

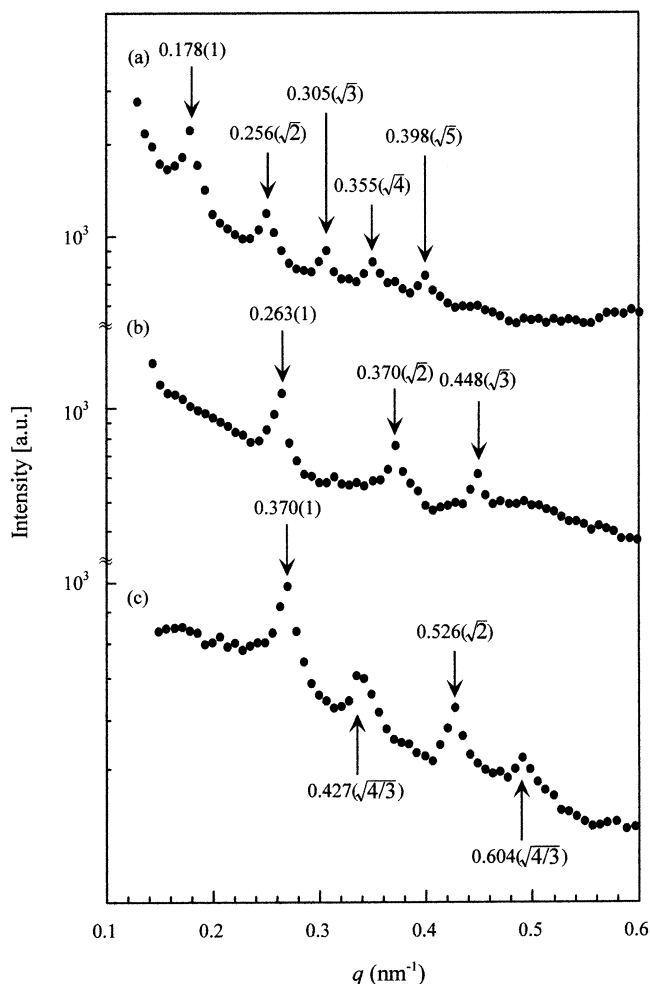
$$D_0 = (1/\sqrt{2})a_c = \sqrt{(3/2)}d_1 \quad \text{for fcc} \quad (2)$$

Table 3 lists the physical values on spatial packing of the cubic lattice for (MS61)<sub>149</sub>F. Figure 4 shows the relationship between  $d_1$  or  $D_0$  and polymer concentration. PEO star takes the disordered state below  $C^*$  (5.5 wt %). Near the  $C^*$ , the star forms the lattice of bcc structure. Beyond ca. 19 wt % of polymer concentration, this structure changes into a mixed lattice of bcc and fcc. Consequently, we carried out the double-logarithmic plot of  $D_0$  as a function of polymer concentration (Figure 5, line a). It is found that the measured  $D_0$  is proportional to the  $-0.30$ th power of the polymer concentration and fits well with the  $-1/3$  power expected for homogeneous system. This fact means that the spherical particles of (MS61)<sub>149</sub>F star lead to isotropic shrinkage with increasing the polymer concentration. The structural ordering of PEO stars is very similar to hierarchical structure transformation of the cubic lattices ob-

**Figure 4.** Relationship between  $d_1$  or  $D_0$  and polymer concentration for (MS61)<sub>149</sub>F.**Figure 5.** Double-logarithmic plots of  $D_0$  as a function of polymer concentration: (a) (MS61)<sub>149</sub>F; (b) (MS61)<sub>37</sub>FI.

served on the core-shell microspheres,<sup>4,5</sup> (AB)<sub>n</sub> stars,<sup>6</sup> and highly branched polyisoprene stars.<sup>7</sup> As mentioned in the Introduction, the core-shell microspheres (two-components system, shell arm number  $f = 116$ ) led to hierarchical lattice transition from bcc to fcc during the film formation.<sup>21</sup> Star polymers as soft sphere take the gradient structure concerning the arm segment density in good solvent. So, this means that the internal structures of star homopolymer with highly branched arms are very similar to those of multicomponent branched such as core-shell microspheres, (AB)<sub>n</sub> stars, and micelles. Our results obtained in this work seem to be reasonable. Recently, Kapnistos<sup>22</sup> and Loppinet<sup>23</sup> reported the crystalline order of high functionality multiarm stars (1,4-polybutadiene arms,  $f = 128$ ). However, they did not observe the ordering phenomena due to a reversible thermal gelation. Such ordering of star polymer may be affected strongly by temperature.

**Structural Ordering of Peripherally Charged PEO Stars.** The structural ordering of peripherally charged PEO stars was also investigated by means of SAXS in aqueous solution. Figure 6 shows typical SAXS



**Figure 6.** SAXS intensity profiles for (MS61)<sub>37</sub>FI: (a) 1, (b) 4, and (c) 23 wt %.

intensity profiles of (MS61)<sub>37</sub>FI. At 4 wt % of polymer concentration (Figure 6b), the first three peaks appear closely at the relative  $q$  positions of  $1:\sqrt{2}:\sqrt{3}$ , as shown in parentheses. These values correspond to the packing pattern of (110), (200), and (211) planes in a bcc structure. In the SAXS profile at 23 wt % of polymer concentration (Figure 6c), the first four peaks appear at the relative  $q$  positions of  $1:\sqrt{4/3}:\sqrt{2}:\sqrt{8/3}$ . These values mean that the structure changed to the mixed lattice of bcc and fcc with increasing the polymer concentration. On the other hand, below the  $C^*$  ( $=4.3$  wt %) (Figure 6a), the first five peaks appear at the relative  $q$  positions of  $1:\sqrt{2}:\sqrt{3}:\sqrt{4}:\sqrt{5}$ , as shown in parentheses. These values correspond to the packing pattern of (110), (200), (211), (220), and (310) planes in a bcc structure.

We also consider special packing of the cubic lattice in aqueous solution. Figure 7 shows the relationship between  $d_1$  or  $D_0$  for the lattice of (MS61)<sub>37</sub>FI and polymer concentration. Below ca. 19 wt % of polymer concentration, the peripherally charged star forms the lattice of bcc structure. Beyond ca. 19 wt % of polymer concentration, the structure changed to the mixed lattice of bcc and fcc. Similar phenomena were observed for (MS70)<sub>72</sub>FI and (MS61)<sub>149</sub>FI. The double-logarithmic plot of  $D_0$  as a function of polymer concentration is shown in Figure 5 (line b). It is found that the measured  $D_0$  is proportional to the  $-0.31$  power of the polymer concentration and fits well with the  $-1/3$  power expected for homogeneous system. This fact means that the

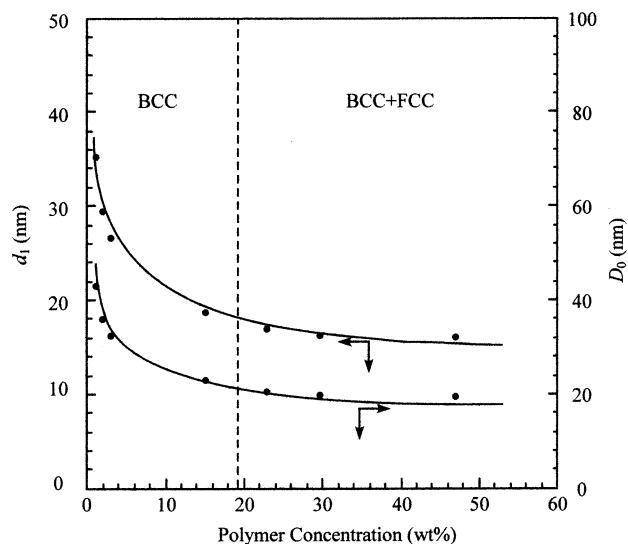


**Figure 7.** Relationship between  $d_1$  or  $D_0$  and polymer concentration for (MS61)<sub>37</sub>FI.

spherical particles of (MS61)<sub>37</sub>FI star lead also to isotropic shrinkage with increasing the polymer concentration. It should also be noticed that the nearest-neighbor distance of the spheres  $D_0$  decreases from 40 to 20 nm by shrinkage with increasing the polymer concentration (1–47 wt %). These values (40–25 nm) are larger than the diameter of (MS61)<sub>37</sub>FI star (see the value of  $R_H = 12.2$  nm listed in Table 2).  $D_0$  seems to be observed with large values by the thickness of electric double layer around the star. With increasing the polymer concentration, the star leads to isotropic shrinkage due to soft sphere, following with decreasing of the Debye screening length in electric double layer. This means that even the peripherally charged star having relatively low branching number leads to the structural ordering by long-range electrostatic repulsions. Thus, peripheral charges affect strongly on the stabilization and structural ordering of amphiphilic stars. More recently, Jusufi and co-workers<sup>24</sup> have presented predictions on the effective interactions of polyelectrolyte stars. They anticipate that a lower critical arm number of ordering will be smaller than the corresponding value 34 obtained for neutral stars. Their prediction agrees with our results. Namely, structural ordering in peripherally charged star polymers for  $f > 37$  was observed, but in functionalized PEO stars (without charges) no such phenomenon was observed.

In general, ionic charges do not dissociate and condense in the presence of inorganic salt. We investigated the structural ordering of (MS61)<sub>37</sub>FI in aqueous solution with the addition of KI. Below ca. 50 mM of KI salt concentration, we also observed the weak ordering. However, such ordering structure changed to disordering, beyond more than 50 mM of KI salt concentration. That is to say, peripherally charged stars behaved as no-charged stars such as (MS61)<sub>37</sub>F in the presence of KI salt. This screening effect is often observed as common behavior in the chemistry of colloid and polyelectrolyte.

#### 4. Conclusions

Functionalized poly(ethylene oxide) (PEO) stars (arm number  $f = 37$ –149) possessing peripheral tertiary amino groups were prepared by organized copolymerization using macromonomers. Subsequently, positive

charges were introduced into such peripheral tertiary amino groups by quaternization. The structural ordering of these functionalized and peripherally charged stars was investigated through SAXS in aqueous solution. Functionalized PEO stars ( $f > 72$ ) formed a bcc structure near the overlap threshold ( $C^*$ ). On the other hand, peripherally charged PEO stars ( $f > 37$ ) formed a lattice of bcc below  $C^*$ . Both stars changed to the mixture of bcc and fcc beyond ca. 19 wt % of polymer concentration. The nearest-neighbor distance of the spheres ( $D_0$ ) decreased continuously with an exponential function increasing the polymer concentration. It was found, moreover, that the measured  $D_0$  was proportional to the  $-1/3$  power of the polymer concentration. This fact meant that the spherical particles of PEO stars led to isotropic shrinkage around high polymer concentration. On the other hand, such structural ordering was observed in peripherally charged stars even below  $C^*$  due to electrostatic repulsion by introduction of peripheral charges. The electrostatic repulsion gave rise to an effective stabilization of stars in aqueous solution. These electrostatic interactions between stars were screened by adding monovalent salt (KI). We are investigating the self-diffusion behavior in aqueous solution via NMR measurements. Investigations are currently under way and will be reported in the near future.

## References and Notes

- (1) Witten, T. A.; Pincus, P. A.; Cates, M. E. *Europhys. Lett.* **1986**, *2*, 137.
- (2) Willner, L.; Jucknischeke, O.; Richter, D.; Farago, B.; Fetters, L. J.; Huang, J. S. *Europhys. Lett.* **1992**, *19*, 297.
- (3) Willner, L.; Jucknischeke, O.; Richter, D.; Roovers, L. J.; Huang, J. S.; Lin, M. Y.; Hadjichristidis, N. *Macromolecules* **1994**, *27*, 3821.
- (4) Saito, R.; Kotsubo, H.; Ishizu, K. *Polymer* **1994**, *35*, 1580.
- (5) Ishizu, K.; Sugita, M.; Kotsubo, H.; Saito, R. *J. Colloid Interface Sci.* **1995**, *169*, 456.
- (6) Ushida, S.; Ichimura, A.; Ishizu, K. *J. Colloid Interface Sci.* **1998**, *203*, 153.
- (7) Ishizu, K.; Ono, T.; Uchida, S. *J. Colloid Interface Sci.* **1997**, *192*, 189.
- (8) Ishizu, K.; Kitano, H. *Macromol. Rapid Commun.* **2000**, *21*, 979.
- (9) Kose, A.; Ozaki, M.; Takano, K.; Kobayashi, Y.; Hachisu, S. *J. Colloid Interface Sci.* **1973**, *44*, 330.
- (10) Nisato, G.; Ivkov, R.; Amis, E. J. *Macromolecules* **1999**, *32*, 5895.
- (11) Oshima, A.; Konishi, T.; Yamanaka, J.; Ise, N. *Phys. Rev. E* **2001**, *64*, 051808.
- (12) Gröhn, F.; Antonietti, M. *Macromolecules* **2000**, *33*, 5938.
- (13) Ishizu, K.; Toyoda, K.; Furukawa, T.; Uchida, S. *J. Colloid Interface Sci.*, in press.
- (14) Ishizu, K.; Shimomura, K.; Saito, R.; Fukutomi, T. *J. Polym. Sci., Polym. Chem. Ed.* **1991**, *29*, 607.
- (15) Furukawa, T.; Ishizu, K. *J. Colloid Interface Sci.* **2002**, *253*, 465.
- (16) Maniruzzaman, M.; Kawaguchi, S.; Ito, K. *Macromolecules* **2000**, *33*, 1583.
- (17) Ishizu, K.; Uchida, S. *Prog. Polym. Sci.* **1999**, *24*, 1439.
- (18) Tsubaki, K.; Kobayashi, S.; Satoh, J.; Ishizu, K. *J. Colloid Interface Sci.* **2001**, *241*, 275.
- (19) Tsubaki, K.; Ishizu, K. *Polymer* **2001**, *42*, 8287.
- (20) Ishizu, K.; Ono, T.; Uchida, S. *Polym.-Plast. Technol. Eng.* **1997**, *36*, 461.
- (21) Ishizu, K. *Prog. Polym. Sci.* **1998**, *23*, 1383.
- (22) Kapnistos, M.; Vlassopoulos, D.; Fytas, G.; Mortensen, M.; Fleischer, G.; Roovers, J. *Phys. Rev. Lett.* **2000**, *85*, 4072.
- (23) Loppinet, B.; Stiakakis, E.; Vlassopoulos, D.; Fytas, G.; Roovers, J. *Macromolecules* **2001**, *34*, 8216.
- (24) Jusufi, A.; Likos, C. N.; Löwen, H. *Phys. Rev. Lett.* **2002**, *88*, 018301.

MA0213807